International Journal of Recent Technology and Engineering (IJRTE)
ISSN: 2277-3878 (Online), Volume-8 Issue-6, March 2020

Radio Frequency Identification (RFID) Integrated System for Security Measures in IoT Applications

Santosh Kumar Upadhyaya

Abstract. This study presents a low frequency RFID (LF-RFID) sensing system integrated with Internet of Things (IoTs) to detect and characterize corrosion. The LF-RFID sensing system comprises of a tag and reader inductively linked with each other. Tag interacts with corroded metal through eddy currents and measure changes in corroded surface conductivity and permeability. Sensitivity and impedance of LF-RFID sensor varies with distance between tag to reader; which is adjusted to find the optimum working range. The static and transient features of LF-RFID sensor signal is used to characterize corrosion at low computational rate. The size of commercial low frequency tags is very small compared to structures in practice. So, IoTs is used to make a wireless sensor network of proposed sensing system. Results showed an enhancement in sensitivity to corrosion characterization at optimum distance between tag and reader. Using IoTs, several sensors are cascaded to make WSN and enable monitoring a wide structural area.

Keywords: LF RFID, Feature extraction, Feature selection, Corrosion characterization, Non-destructive testing and evaluation (NDT&E)

I. INTRODUCTION

Metals corrode due to their reaction with surrounding environments [1]. Paint coatings of various chemicals are normally used to prevent its occurrence. However, this is not a permanent solution and the paint coated metallic structures can corrode with age. Several research studies and equipment have been developed and/or are in progress for its early detection and estimation. For example, electrochemical impedance spectroscopy (EIS) [2] and electromagnetic non-destructive testing and evaluation (NDT&E) methods such as eddy current (EC) and pulsed eddy current (PEC) techniques [3-4]. These techniques are conceptually based on measuring the reduction in conductivity and permeability of corroded area [5-6].Their measured signals are normally analyzed through feature extraction techniques to detect and characterize corrosion [7-8].

The existing NDT&E techniques have wide applications; however, these are still associated with several shortcomings [9]. For example, the sensitivity of EC and PEC techniques decreases significantly with increasing lift-off distance between their probe and sample surface under investigation. In addition, the majority of existing techniques are limited to use for real time monitoring of metal surface because of their size, operational complexity and cost of instrumentation. Moreover, the existing technologies can only monitor the size of corroded surface equal to the size of sensor. However in practice, the corroded surface area can be comparatively very large. So, existing techniques needs to be repetitively used to cover the corroded area, and are thus expensive in both time and cost. Therefore, this paper exploited a combination of low frequency RFID tags and IoTs for detecting and characterizing corrosion. This is because these are cheap, passive and can be permanently embed into structures for long term monitoring [9,10].To extend the monitoring area, a series of LF-RFID sensors are connected using FRDM-K64F IoT kit to develop a wireless sensor network for monitoring a large area in one time. In the proposed IoT-LF-RFID system, the tags are placed on metallic surface to be tested. The response of these tags is measured at reader sequentially, and its monotonic features is extracted and used to detect and characterize corrosion [10, 11]. The principle of LF-RFID sensing system is detailed below.

1. Modelling LF-RFID Based Corrosion Sensing System

The proposed IoT-LF-RFID corrosion sensing system is shown in Fig. 1.1. The sensor part consists of two hardware components: reader and tag. The reader primarily consists of RF circuitry to transmit and receive 125 KHz (low frequency RFID) RF energy to power and communicate with tag. The tag is passive and placed on the metal surface to be investigated. The reader transmits 125 KHz RF signal to power the tag. In return, the tag backscatters the code stored in its memory to reader. This response signal is measured at reader and its monotonic features is extracted and used to detect and characterize corrosion [10, 11]. The concept of eddy currents models interaction between tag and corroded metal, whereas, inductive coupling establishes communication link between tag and reader.

Manuscript received on March 15, 2020.
Revised Manuscript received on March 24, 2020.
Manuscript published on March 30, 2020.
* Correspondence Author
Santosh Kumar Upadhyaya*, Cisco Systems, Senior Technical Leader, Cisco Systems, Senior Technical Leader

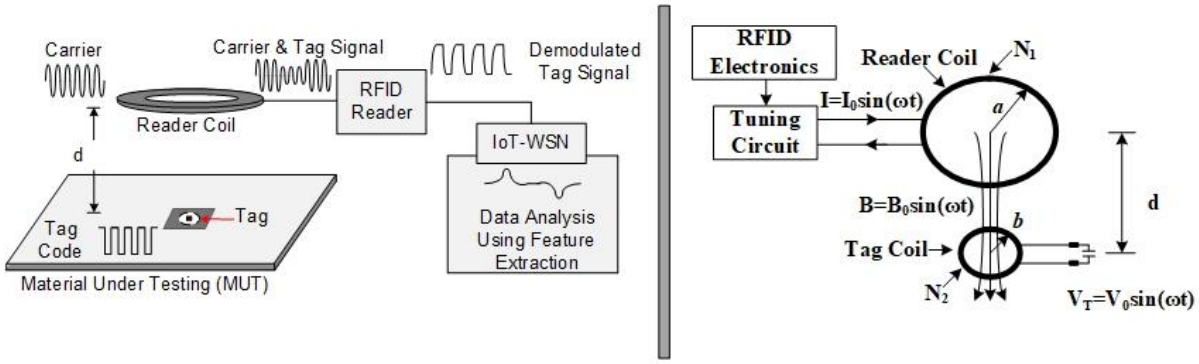

Fig. 1.1 Functional block diagram of LF-RFID corrosion sensing system.

The electrical equivalent model of developed LF-RFID sensing system is presented in Fig. 13.2. The tag and reader is represented by L-C-R circuit. The metal is conductive in nature, so it is represented as L-R circuit. The metal near or in contact of tag is modelled as an additional parallel inductor with self–inductance (L_M) and resistance (R_M). In the absence of metal (Fig. 1), the voltage (V_T) induced in tag is governed by magnetic field passing through the entire surface (S) of tag coil, as:

$$V_T = \frac{\pi \mu_0 I f N_1 N_2 S a^2 \sqrt{L_T}}{R_T \sqrt{C_T (a^2+d^2)^3}} \cos(\alpha) \quad (1)$$

where, d =co-axial distance between reader and tag coils,

μ_0= permeability of free space and is $4\pi * 10^{-7}$ Henry/meter,

$N_1 N_2$= number of turns in reader coil and tag coil respectively,

a and b= radius of reader and tag coil respectively;

f= frequency of the RFID carrier signal; S = area (m2) of tag coil,

R_T and L_T= resistance and self-inductance of tag coil respectively.

From (1), the induced voltage (V_T) in tag depends upon the angle (α) between B and S, and the relative tag to reader distance. Therefore, the two coils (reader and tag coil) are placed in parallel $(\alpha = 0)$ to each other to pass maximum magnetic flux. Equation (1) also indicate that the voltage (V_T) induced in tag coil depends on the coil physical (e.g. number of turn and area) and electrical parameters, and the relative position of tag with respect to reader coil. This paper exploited commercial RFID tags, so tag coil parameters (such as dimension, shape and number of turns) were limited to change. Therefore, from (1), the relative tag to reader distance was adjusted to match impedance and to improve sensitivity.

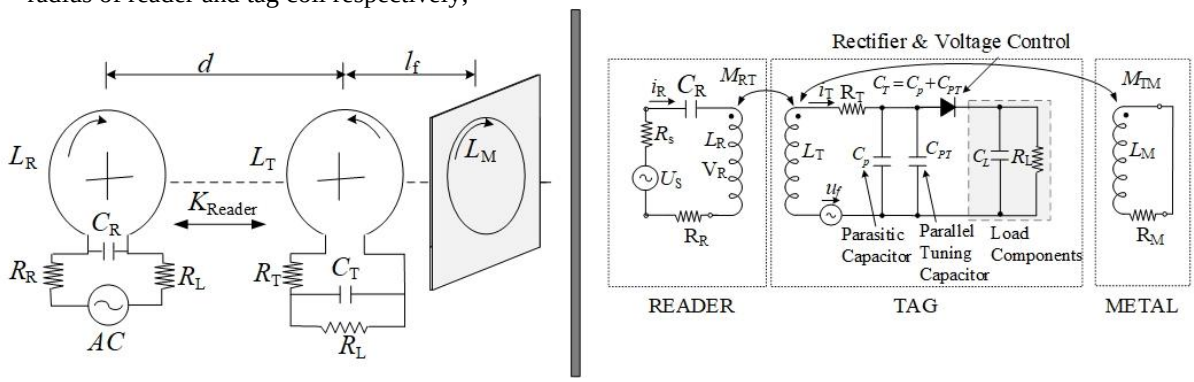

Fig. 1.2 Electrical equivalent model of proposed LF-RFID corrosion sensing system showing

inductive coupling between reader, tag and metal.

2.1 LF-RFID sensing system and corrosion

To model the effect of metal and corrosion, the voltage (V_R) across reader coil with inductance (L_R) and in the absence of metal is computed using Fig. 2 as:

$$V_R = L_R \frac{di_R}{dt} \pm M_{RT} \frac{di_T}{dt} \quad (2)$$

where, i_R and i_T represents the current flowing in reader and tag coil respectively. M_{RT} is the mutual inductance between reader and tag. Similarly, the tag voltage (V_T) across load can be expressed as:

$$V_T = L_T \frac{di_R}{dt} \pm M_{RT} \frac{di_T}{dt} + i_T R_T \quad (3)$$

where, L_T and R_T represents the respective inductance and resistance of tag coil. In Fig. 1.2, the presence of metal as an additional parallel inductor will reduce tag's overall inductance, and thus impedance and sensitivity. This will change current (i_T) and readercoil voltage (V_R), as governed by (2) and can be measured through feature extraction. To model the effect of corrosion, it is considered that the resistance (R_M) and inductance (L_M) of metal depends upon its physical properties, e.g., dimensions, conductance and permeability. These properties changes as the corrosion progresses with time.

Variation in parameters (L_M and R_M) changes the impedance of LF-RFID sensing system, which can be measured as a monotonic change (increase or decrease) in features of LF-RFID signals. Next section will explain various features of measured signal of LF-RFID sensing system and their sensitivity to corrosion characterization.

3 Feature Extraction And Selection To Characterize Corrosion

In the absence of any metallic structure, the response of LF-RFID sensing system should be ideally in the form of square wave pulses, given by (1). However, its shape changes when the tag is placed in proximity of metal. This phenomenon is due to eddy currents and impedance mismatch. An example of its shape when tag was placed on a metal is shown in Fig. 1.3.

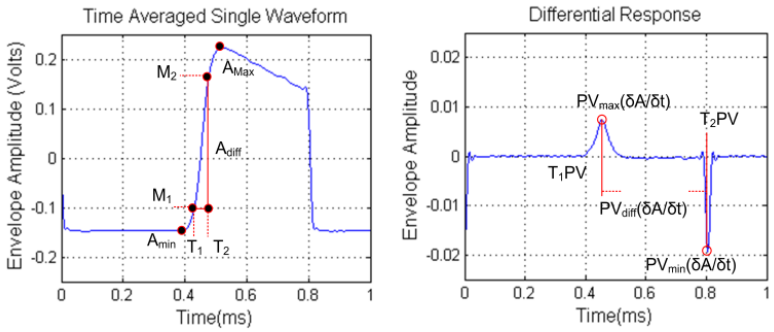

Fig.1. 3. An example of the measured response of LF-RFID sensing system and its differential showing the transient features. The tag was placed on the non-corroded metallic surface.

In Fig. 3, the response is not a perfect square wave and has variations in both top and transient sides. These variations carry information about corrosion and crack on metal surface. This information can be characterized through feature extraction, similar to PEC NDT technique. It is because the wave shape in Fig. 1.3 is similar to PEC NDT technique; which has been widely used to characterize defects on metals through feature extraction [6, 7]. Some already studied features include amplitude, duty cycle, zero crossing and rising edge[6, 7]. In this paper, two time domain static and transient features of LF-RFID sensor signal have been explored. These features are selected as these are already proven to be robust and give repeatable results to integrate the LF-RFID system with IoT kit. The static and transient features are shown in Fig. 1.3.

To explain features, the measured signal is denoted as A in Fig. 1.3. The first static feature (A_{max}) represents the maximum value of pulse A and characterizes the permeability variation. The other static features used for comparison are: A_{diff} and A_{edge}. Feature A_{diff} represents the difference between maximum and minimum of pulse A. Feature A_{edge} represent the rising edge of pulse and is defined by the upper (M_2) and lower (M_1) threshold of rising edge. Transient features were computed by taking the first derivative ($\delta A/\delta t$) of signal (A), as shown in Fig. 3. The transient feature of interest is $PV_{max}(\delta A/\delta t)$, which represents the maximum peak value of $\delta A/\delta t$. It reflects the variation (reduction) in conductivity of corroded metal with increase in thickness of corrosion layer. Other transient features used for evaluation and comparison include $PV_{min}(\delta A/\delta t)$ and $PV_{diff}(\delta A/\delta t)$. Feature $PV_{min}(\delta A/\delta t)$ represents the minimum peak of $\delta A/\delta t$. Finally, the feature $PV_{diff}(\delta A/\delta t)$ represents the difference between maximum and minimum of differential signal peak. These features are experimentally evaluated in next section.

II. SAMPLE DESIGN AND EXPERIMENTAL SETUP

The progress of corrosion layer in metal varies non-uniformly with time. It is due to variations in proportion of its constituents (iron oxides and hydroxides) with time and atmosphere surrounding the metal. This paper focuses on early stage corrosion, when the thickness of corrosion increases with time. However, in long-term corrosion, it tends to decrease due to metal loss. For this study, the samples used are shown in Fig. 13.4.

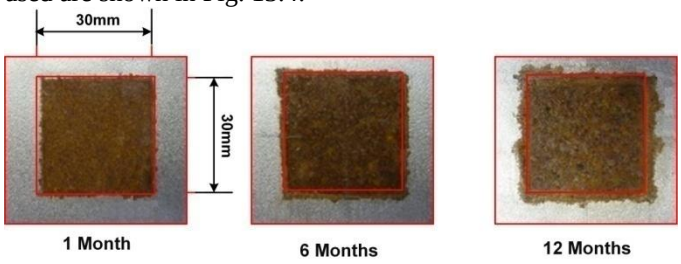

Fig. 1.4. Images of corrosion patches on the samples.

The corrosion samples are made up of several mild steel plates of various sizes. For example, the plates in Fig. 4 have dimensions of 200 × 80 × 5 mm(length × width × thickness). To prepare the corrosion samples, a rectangular patch (e.g. 30mm × 30mm in Fig. 13.4) on plate was left exposed to corrode. The rest of plate was covered with plastic tape to keep the steel clean and dry. The atmospheric exposure duration was of 1, 6and 12 months to develop different level of corrosion. An example of developed corrosion patches is shown in Fig.1. 4.For larger corroded area patches, 16 sensors are connected in a matrix of 4 by 4.For these multiple connected sensors using IoTs, the multiple signals are obtained sequentially and are assessed individually. The developed LF-RFID based sensor, IoT kit and the developed algorithms to integrate a sequence of 16 LF-RFID sensors to IoT kit in order to locally pre-process information and then transmitting the processed information to base station is shown in Fig. 13.5.

In the test setup shown in Fig. 5, the tag used was programmed with code consisting of all '1's 'at a data bit rate of 125KHz/32 = 3.906KHz with 50% duty cycles.

The selection of all '1's 'was made because it resulted into uniform stream of square pulses and thus its averaging can be easily performed at the IoT node. Each tag was placed on the corrosion patch to be monitored. The relative position and alignment of the reader coil, tag and corrosion patch was maintained throughout the experiments. Readings were taken for a reader tag relative spacing of 0mm, 10mm, 20mm and 30mm.

The reader circuit was designed for reading the signals, as shown in Fig. 1.1. In the reader, the measured signal was firstly demodulated and filtered to remove the 125 KHz carrier and noise. This was done by a diode based envelope detector followed by an op-amp based filter and buffer. The filtered output signal was then digitized using FRDM-K64F IoT base module. The reader coil in Fig. 1.5 was designed of circular shape with 35 mm in diameter, so that most of the RF energy produced by reader coil spreads over space limited to the area of tag. The reader coil had resistance R = 11.35 Ω and inductance L = 738µH. For these parameters, the reader and tag had theoretical resonant frequency of 125 KHz in free space. The system was calibrated for this frequency by adjusting the distance between tag reader. The experimental outcomes are discussed below.

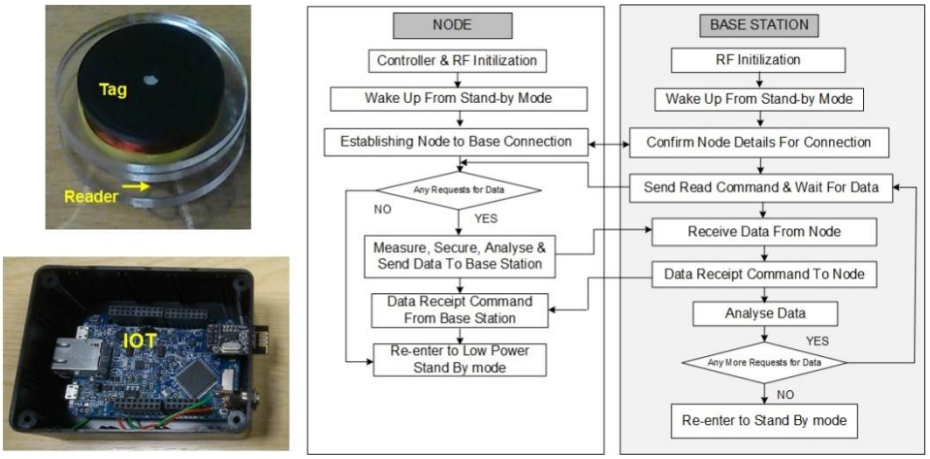

Fig. 1.5. The developed LF-RFID based sensor, IoT board and the simplified representation of the developed IoT-LF RFID node to base interaction algorithm.

III. RESULTS & DISCUSSION

To evaluate the developed IoT-LF-RFID sensing system, two stages of experiments (impedance matching and corrosion characterization) were carried out. The tests were carried out for stand-off distances of 0, 10, 20 and 30mm between tag and reader. The measurements were repeatedly taken 10 times for each sample and relative tag reader distance of 0, 10, 20 and 30mm. The outcomes are discussed below.

5.1 Impedance vs distance

In the proposed LF-RFID corrosion sensing system, the impedance was matched by adjusting the distance between tag and reader coils. For this purpose, the frequency of RFID carrier signal was changed from 116KHz to 132KHz. This was repeated for each corroded sample and tag-reader spacing of d=0, 10, 20 and 30mm. The LF-RFID sensor signal was measured at reader for each carrier frequency, sample and spacing, and is shown in Fig1. 6. The amplitude of measured signals was found varying with the distance between tag and reader, due to change in impedance. Therefore, for each sample and spacing, the maximum amplitude of measured signal and its corresponding carrier frequency was computed. This carrier frequency gives the resonant frequency of system at which impedance matches. This is reported in Table I for all the samples and tag-reader spacing used. The highest resonant frequency measured close to theoretical resonance frequency (125 KHz) is marked in Table 1.1 for each distance and discussed below.

TABLE 1.1:RESONANT FREQUENCIES OBTAINED FOR DIFFERENT TAG READER SPACING

CORROSION SAMPLE	Relative Tag Reader Spacing (mm)			
	0	10	20	30
1	123.125	121.2500	123.125	124.9850
6	123.125	121.2500	123.125	125.0000

12	123.125	121.2500	123.125	124.9850

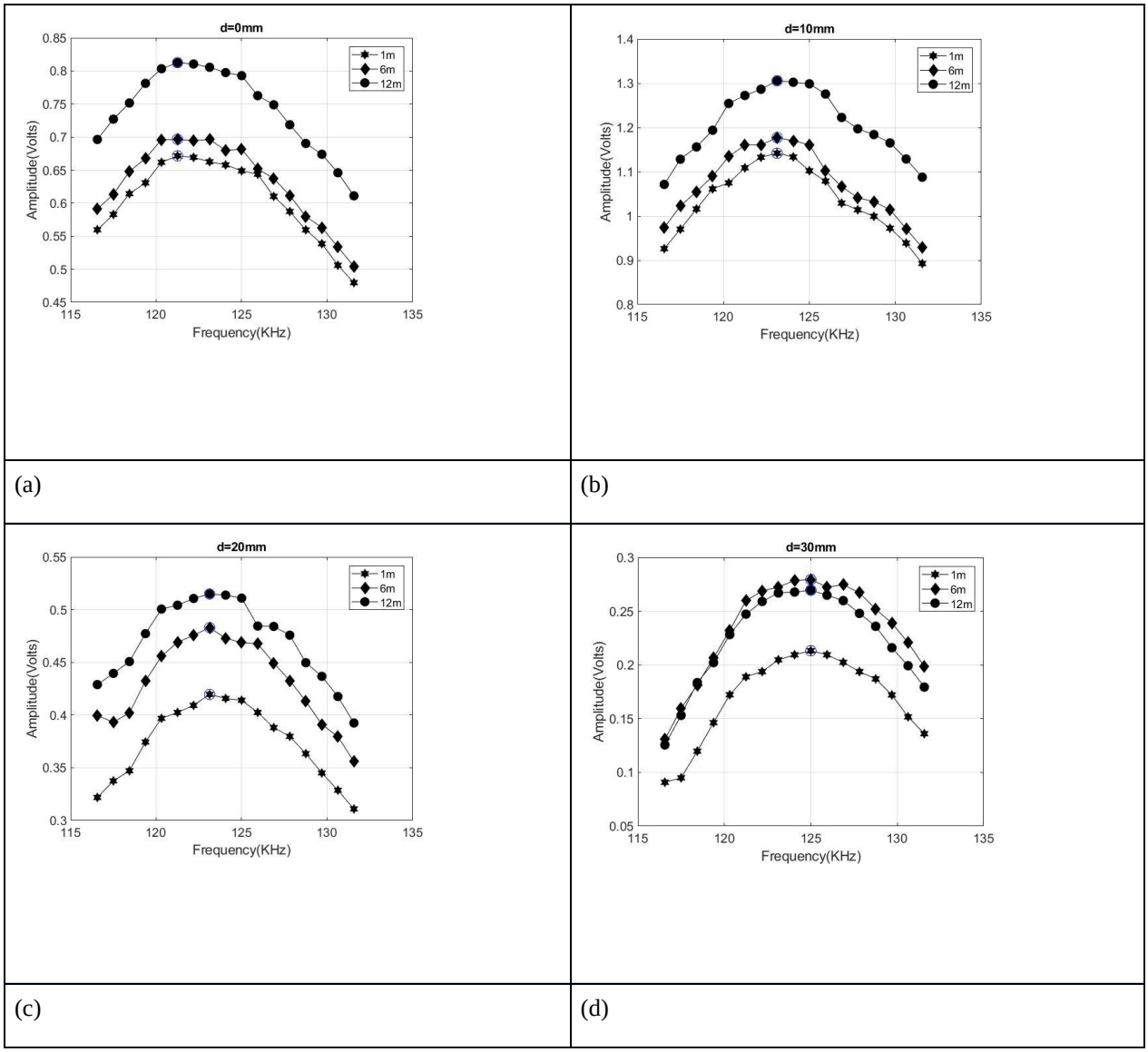

Fig. 1.6. Resonance frequency calculations for tag-reader spacing (a) d=0mm, (b) d=10mm, (c) d=20 mm and (d) d=30 mm. The signals were measured for corroded samples with corrosion exposure duration of 1, 6 and 12 months.

For d=0, 10 and 20mm in Fig 1.6, a significant variation from theoretical resonant frequency (125 KHz) was obtained. This is because for these distances, the influence of reader coil dominated over the flux produced by tag. Therefore, the measured signal from reader for this range contains little or no information regarding the interface between tag and corroded metal. For d=30mm (Fig. 1.6d), the resonant frequency matched more closely to the theoretical value of 125 KHz for each sample.

To confirm, tests were repeated for the carrier frequency of 125KHz and the tag reader spacing of 0, 10, 20 and 30mm. The LF-RFID sensor signal was measured and its static (A_{max}) and transient feature (PV_{max}) were extracted and shown in Fig. 1.7. For d=0, 10 and 20mm, the monotonic trend was found not progressively increasing in accordance with the corrosion exposure duration from 0 to 12 months. It is because the signal amplitude obtained at 125KHz resonant frequency was not found increasing in accordance with the age of corrosion. However, for d=30mm, a monotonically increasing response can be seen in Fig. 1.7.It is because for this distance (d=30mm), the impedance is matched in presence of non-corroded metal. This is discussed in next section through more detailed results obtained at resonant frequency.

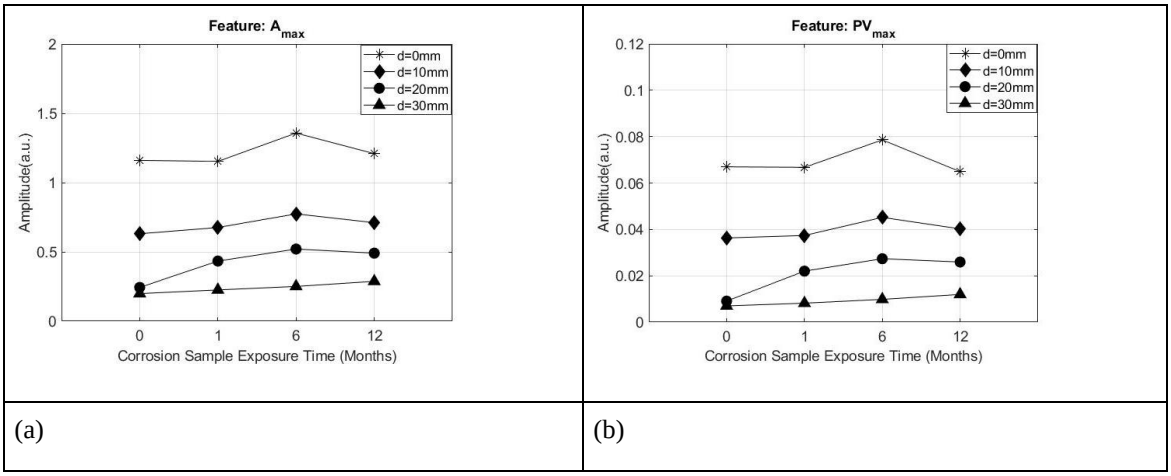

(a) (b)

Fig. 1.7. Features (a) A_{max} and (b) PV_{max} variation for corroded metal samples of 1, 6 and 12 months and tag reader relative spacing of 0, 10, 20 and 30mm.

IV. CORROSION CHARACTERIZATION THROUGH FEATURE EXTRACTION

The selection of most sensitive and robust feature is done using the relative variation (ε), which refers as the percentage difference relative to same feature of sample with less corrosion exposure duration. For example, the relative variation for sample 6 and sample 1 is calculated as follows:

$$\varepsilon = \frac{feature of sample 6 - same feature of sample 1}{value of feature of sample 1} * 100 \quad (4)$$

The results for relative variation are compared in Table II for the six features. For simplicity, an example of samples 1 and 6 is given in Table II. Other samples were also analyzed similarly. The computed six features are divided in two groups: static and transient features, and are shown in Fig 8. The relative tag reader spacing was set to d=30mm (resonant) and carrier frequency to 125 KHz. The selection of d=30mm was made from the results obtained in previous section; where, the impedance of sensing system was found to be matched at this position.

From the theoretical discussions made above, the proposed LF-RFID corrosion sensing system should show a monotonic change in features with exposure duration, provided the impedance is matched. The same can be seen in Fig 8; where, the measured features show a monotonically increasing trend with exposure time. The error bars are very low showing lower uncertainty of data and an increased accuracy and robustness. However, this monotonic response increased non-uniformly with time. It is because the corrosion grows non-uniformly with time and so does its properties. The performance of features is evaluated using the relative variation mentioned in Table II. The static feature (A_{max}) characterize the permeability change; whereas, transient feature ($PV_{max}(\delta A/\delta t)$) characterize the conductivity variation. The transient feature ($PV_{max}(\delta A/\delta t)$) show higher sensitivity than the static features. Other features also vary in the same monotonic pattern as can be seen in Fig 13.8, and thus prove the robustness of system and may be useful in future for other applications.

TABLE 1.2:FEATURES EVALUATION FOR 6 MONTH AND 1 MONTH CORRODED SAMPLE

Static Feature	Sample 6	Sample 1	(%)	Transient Feature	Sample 6	Sample 1	(%)
A_{max}	0.2568	0.2255	13.8827	$PV_{max}(\delta A/\delta t)$	0 .011	0.0082	43.90
A_{diff}	0.4206	0.3730	12.7614	$PV_{min}(\delta A/\delta t)$	0.027	0.0196	37.75
A_{edge}	0.3809	0.3357	13.4644	$PV_{diff}(\delta A/\delta t)$	0 .031	0.0278	14.38

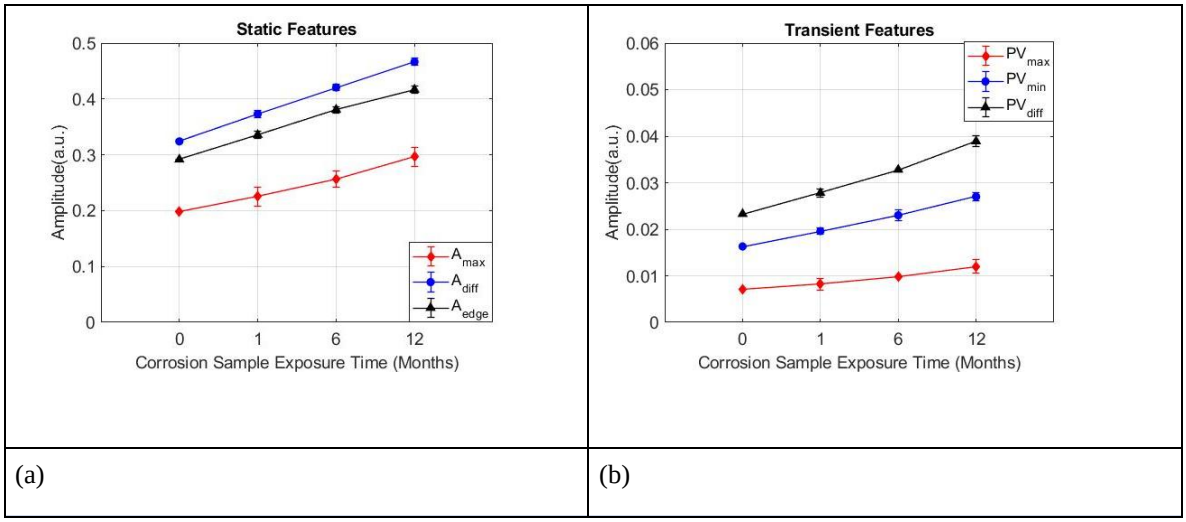

(a) (b)

Fig. 1.8. Comparison of (a) static and (b) transient feature variation for corroded metal samples of 1, 6 and 12 months and tag to reader relative spacing of 30mm.

V. CONCLUSION AND FUTURE WORK

This paper presented and evaluated an IoT-LF-RFID corrosion sensing system. The system is flexible, as the distance between tag and reader can be adjusted to match impedance and thus attain the optimum working range. However, this working range may vary with the type of tag. For the tag used, a 30mm separation distance between tag and reader is found to be the closest optimum distance to match impedance, when tag is placed on the mild steel sample. At this distance, the sensitivity and accuracy of LF-RFID sensing system was found to be significantly increased. This is because at lower stand-off distances (d<=20mm), the influence of reader coil dominated the tag and the monotonic change in features was not obtained. However, at higher stand-off distances (d>30mm), the tag coil do not receive enough power from the reader coil; thus, reducing its sensitivity to corrosion.

To characterize corrosion, six features of LF-RFID sensor output were extracted and compared. Among these features, two features: static (A_{max}) and transient ($PV_{max}(\delta A/\delta t)$) were selected to respectively determine permeability and conductivity changes with corrosion exposure. From selected features, transient responses have proven to be significantly more sensitive and robust with corrosion progression compared to conventional static features. In nutshell, the IoT-LF-RFID sensing system is capable of detecting and characterizing corrosion through feature extraction. Future work will focus on designing miniaturized system suitable for industrial applications.

REFERENCES

1. P.A. Schweitzer. (2003, June, 26). *Metallic Materials: Physical, Mechanical, and Corrosion Properties.* Marcel Dekker, New York.
2. M. Hattori, A. Nishikata and T. Tsuru. (June, 2010). EIS study on degradation of polymer-coated steel under ultraviolet radiation. *Corrosion Science. 52 (6).* pp. 2080-2087.
3. G. Y. Tian, A. Sophian, D. Taylor and J. Rudlin (Feb., 2005). Multiple sensors on pulsed eddy-current detection for 3-D subsurface crack assessment. *IEEE Sensors Journal.*5(1). pp. 90-96.
4. M.E. Davoust, L. Le Brusquet and G. Fleury (September 2010). Robust estimation of hidden corrosion parameters using an eddy current technique. *Journal of Nondestructive Evaluation.* 29 (3). pp. 155–167.
5. Y. He, F. Luo and M. Pan (November, 2010). Defect characterisation based on pulsed eddy current imaging technique. *Sensors and Actuators A: Physical. 164 (1-2).* pp. 1–7.
6. G.Y. Tian and A. Sophian. (January, 2005). Defect classification using a new feature for pulsed eddy current sensors. *NDT & E International.38 (1).* pp. 77–82.
7. T. Chen, G.Y. Tian, A. Sophian and P.W. Que. (September 2008). Feature extraction and selection for defect classification of pulsed eddy current NDT. *NDT & E International*. 41 (6). pp. 467–476.
8. R.A. Smith and G.R. Hugo. (January, 2001). Transient eddy current NDE for ageing aircraft capabilities and limitations. *Insight-Non-Destructive Testing and Condition Monitoring*. 43(1). pp. 14–25.
9. D. Fuente, I. Diaz, J. Simancas, B. Chico and M. Morcillo. (February, 2011). Long-term atmospheric corrosion of mild steel. *Corrosion Science*. 53 (2). pp. 604–617.
10. M. Alamin, G.Y. Tian, A. Andrews and P. Jackson (February, 2012). Corrosion detection using low-frequency RFID technology. *Insight Non-Destructive Testing and Condition Monitoring*. 54 (2). pp. 72–75.
11. A. I. Sunny, G. Y. Tian, J. Zhang, M. Pal (April, 2016). Low frequency (LF) RFID sensors and selective transient feature extraction for corrosion characterisation. *Sensors and Actuators A: Physical*. 241. pp. 34-43.

AUTHOR PROFILE

Santosh Kumar Upadhyaya,
Master in Software Systems from BIT, Pilani.Cisco Systems, Senior Technical Leadersantosh.hkd@gmail.com 9880599455
Around 20 years of experience in IT industry.
Experience in network security products and authentication, authorization and accounting frame work.